33RD INTERNATIONAL SYMPOSIUM ON BALLISTICS
BRUGES, BELGIUM, OCTOBER 16–20, 2023

ON THE BALLISTIC IMPACT RESISTANCE OF ADDITIVE MANUFACTURED MARAGING STEEL TARGETS COMPARED TO THAT OF CAST TARGETS

Maisie Edwards-Mowforth[1], Miguel Costas[2], Martin Kristoffersen[2], Filipe Teixeira-Dias[1] and Tore Børvik[2]

[1]*Institute of Infrastructure and Environment (IIE), School of Engineering, The University of Edinburgh, UK*

[2]*Structural Impact Laboratory (SIMLab), Department of Structural Engineering, NTNU – Norwegian University of Science and Technology, Trondheim, Norway*

The advent of additive manufacturing (AM) in the defence industry has introduced possibilities for customisable and optimised light-weight armour. Maraging steel is well suited to AM and takes on ultra high-strength post heat-treatment, lending it significant potential for protective applications. Promising ballistic performance has been demonstrated in the literature albeit with a tendency for brittle behaviour; it remains unknown to what extent the AM process is responsible for the unfavourable strength versus ductility trade off. Here, AM maraging steel in both the as-printed and heat-treated state has been experimentally characterised, examined, and tested in a ballistic range alongside its traditionally cast counterpart. Very little difference was found in the ballistic limit velocity of the AM maraging steel compared to cast both before and after heat treatment, despite a dramatic reduction in ductility. In the majority of the ballistic impact tests, damage inflicted on the projectile core was more extensive for the AM targets than for the cast.

INTRODUCTION

Flexible and customisable production, one-off parts and even on-site armour repairs are examples of the possibilities offered by the use of additive manufacturing (AM) in defence applications. Laser powder-bed fusion (LPBF) processes in particular enable the building of intricate metallic parts with complex multi-scale geometries that may be utilised for armour with high strength-to-weight ratios. The uncertainty related to the effect of AM material properties on ballistic performance, however, has meant that the application of AM techniques to advance protective structures is as of yet unrealised [1, 2]. To date, existing studies have found promisingly little difference between the ballistic performance of AM aluminium compared to cast material of the same composition [3], and attempts have been made to modify AM processing parameters for optimised ballistic performance of titanium targets [4, 5].

Maraging steel is a martensitic steel that takes on ultra high-strength post heat-treatment and is commonly used in aerospace industry [6]. The low carbon composition of maraging steel makes it suited to manufacturing through LPBF: the strengthening intermetallic precipitates developed during cyclic heating and subsequent heat-treatment may cause cracking in high-carbon steels [7, 8]. It is well established that high mechanical strength correlates with favourable ballistic performance [9, 10]. As such, significant potential for AM maraging steel in protective applications was demonstrated in initial experimental studies by Costas et al. [11]. However, a tendency for brittle fracture became evident with a detrimental effect on ballistic performance for heat-treated AM maraging steel.

A reduction in ductility associated with high-strength can cause fragmentation and erratic behaviour of targets under ballistic impact and reduce the overall perforation resistance [9, 12, 13]. At the same time, LPBF process defects such as lack of fusion between melt track layers and unmelted powder are known to induce anisotropy, in particular in the fracture strain [7, 11]. It remains unclear to what extent the additive manufacturing process is responsible for the unfavourable strength versus ductility trade off for AM maraging steel targets. The performance of AM maraging steel alongside traditionally cast maraging steel under the same experimental ballistic test conditions has not yet been examined.

In this study, AM maraging steel in both the as-printed and heat-treated state has been experimentally characterised and tested in a ballistic range alongside its cast counterparts. Comparisons of ballistic performance are informed by the mechanical properties disclosed in quasi-static tensile tests, the ballistic limit velocities, and the observed microstructures of different target material configurations. Scanning electron microscope (SEM) images were taken to shed light on fracture surfaces and penetration channels, and high-speed cameras recorded the ballistic impact tests to observe perforation mechanisms at play.

The AM maraging steel had a marginally lower ballistic limit velocity compared to that of the cast maraging steel both before and after heat treatment, despite exhibiting a far smaller strain at fracture that was dramatically reduced after heat-treatment. Both the heat-treated AM and cast maraging steel demonstrated a capacity to pulverise the armour piercing bullet upon impact at the ballistic limit velocity. However, in the majority of impact tests, damage inflicted on the hard steel bullet core was more extensive for the AM material than for the cast material.

EXPERIMENTAL METHODOLOGY

AM and cast maraging steel specimens were manufactured for an experimental campaign to disclose the mechanical characteristics and ballistic performance. All cast maraging steel specimens were machined from a Ø60.5 $\times$ 500 mm cylinder provided by Abrams steel [14]. Six AM maraging steel cylinders of Ø60.5 $\times$ 50 mm were produced using LPBF with the island scan strategy as detailed in Figure 1 using a 200 W Concept Laser M2 and processing parameters listed in TABLE I. Specimens for tensile tests and target plates for ballistic impact tests were machined from the cylinders to the specifications in Figure 1. Note that tensile specimens for the AM material were extracted with orientation in the build-direction, indicated by the z direction in Figure 1. The build direction is expected to represent the worst

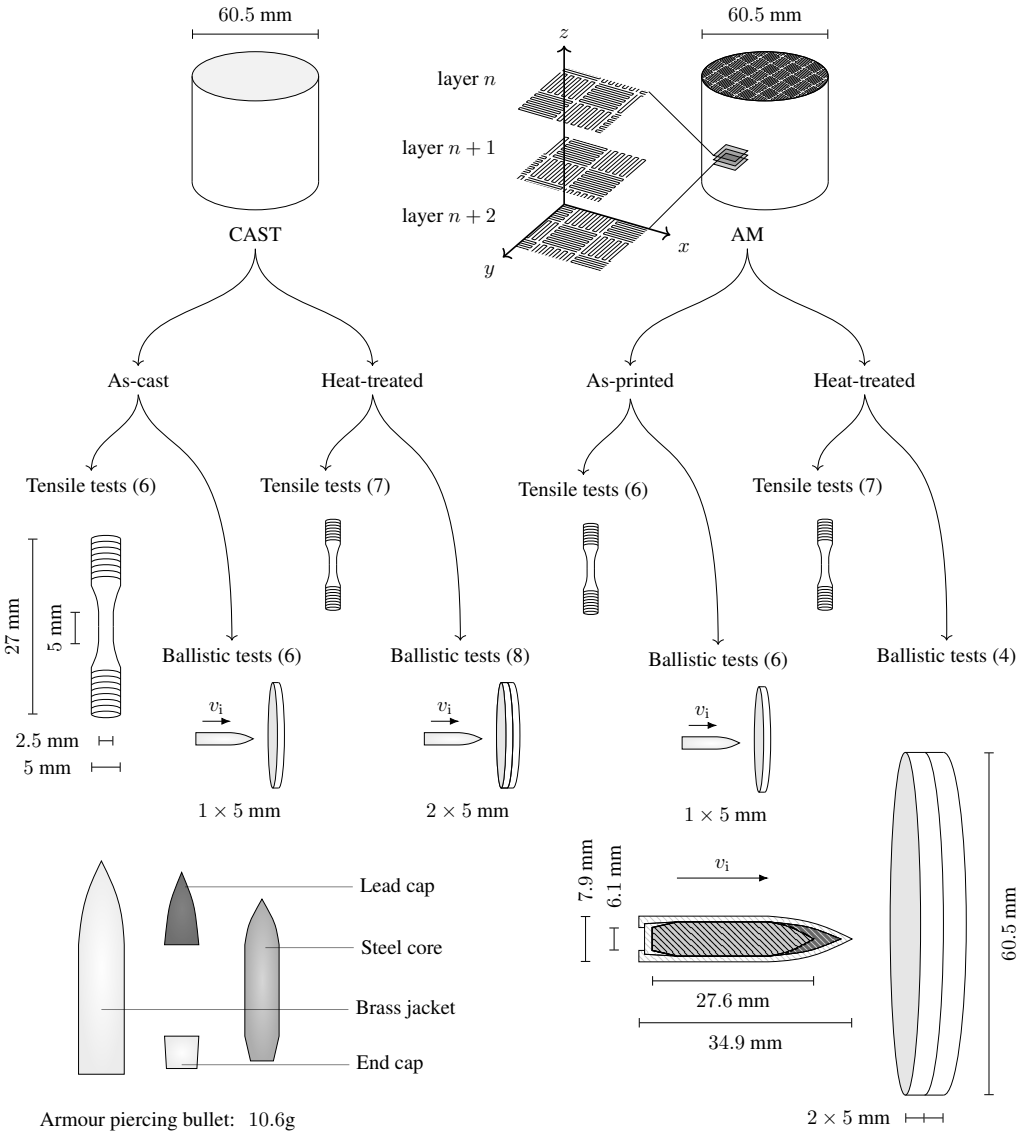

Figure 1. Schematic of experiments and maraging steel specimen details with the number of tests listed in brackets.

case scenario for reduced ductility due to AM processing as demonstrated by Costas et al. [11]. Half of the specimens were tested in their as-printed or as-cast state, while half underwent industry standard heat-treatment of $490\,^{\circ}\mathrm{C}$ for 6 hours followed by air cooling.

Quasi-static uniaxial tensile tests were carried out using an Instron universal testing machine with an initial strain rate of $1 \times 10^{-3}\ \mathrm{s}^{-1}$. Two synchronised Basler cameras captured the tests at 3–10 frames per second which were analysed with the digital image correlation software eCorr [15]. The Cauchy (true) stress, σ_t, and logarithmic strain, ϵ, were computed using

$$\sigma_\mathrm{t} = F/A \tag{1}$$

and

$$\varepsilon = \ln\left(A_0/A\right) \tag{2}$$

TABLE I. ADDITIVE MANUFACTURING PROCESS PARAMETERS.

Laser power	Layer thickness	Laser velocity	Focus diameter	Hatch distance	Powder size
180 W	30 µm	600 mm/s	150 µm	105 µm	$10 - 45$ µm

respectively, where F is the force recorded by the load cell, A is the specimen gauge area, and A_0 is the initial cross-section area of the gauge area.

The ballistic limit velocity, v_{bl}, was disclosed by firing 7.62 mm calibre armour piercing projectiles at target plates in a ballistic range using a smooth-bored Mauser rifle as described by Børvik et al. [9]. Projectile impacts from 300–1000 m/s against targets secured in a circular clamp were recorded at 300,000 frames per second by a Phantom high-speed TMX 7510 camera to measure initial, v_{i}, and residual, v_{r}, velocities. The Recht-Ipson model [16] was fitted to the experimental data using the least squares method to estimate v_{bl} for each target configuration. The Recht-Ipson model is given as

$$v_{\mathrm{r}} = a(v_{\mathrm{i}}^{p} - v_{\mathrm{bl}}^{p})^{1/p} \tag{3}$$

where a and p are constants fixed at 1 and 2, respectively, for the purpose of forming grounds for comparison between target materials. Note that the intention of this study is to draw comparison between AM and cast maraging steel for non heat-treated and heat-treated states separately. Results of experimental ballistic impact tests on the as-printed and heat-treated material are not directly comparable due to different target thicknesses used (1×5 mm cast targets and 2×5 mm AM targets as shown in Figure 1).

RESULTS

Material Characterisation

Results from the quasi-static tensile tests and ballistic impact tests are reported in Figures 2a and 2b respectively. The expected improvement in mechanical strength after heat-treatment of maraging steel manifested as an increase in both the yield stress, σ_{y}, and ultimate tensile strength, S_{UTS}, of approximately 60% and 80% for the AM and cast, respectively. Alongside increased strength, a worsened strain-capacity after heat-treatment was evidenced by a reduction of 30–40% in strain at peak force, e_{UTS}, and a reduction of approximately 48% and 93% in strain at fracture, ϵ_{frac}, for the cast and AM maraging steel respectively.

Figure 2b presents the ballistic limit curves for the 1×5 mm cast targets and 2×5 mm AM targets both before and after heat-treatment. Very little scatter is observed in the data for the as-printed targets with only slightly more for the heat-treated targets. As expected, the ballistic limit velocity of the doubled AM heat-treated targets demonstrated a far higher ballistic limit than the non heat-treated single targets. The differences found in ballistic limit velocity between AM and cast maraging steel were small both before and after heat-treatment. Before heat-treatment, the AM targets were found to possess a ballistic limit velocity approximately 5% lower than that of the cast targets, while after heat-treatment ballistic limit velocity of the AM targets was 4% lower than cast.

Features that typically characterise ductile and brittle failure can be identified for the as-printed and heat-treated maraging steel, respectively, in SEM images of tensile

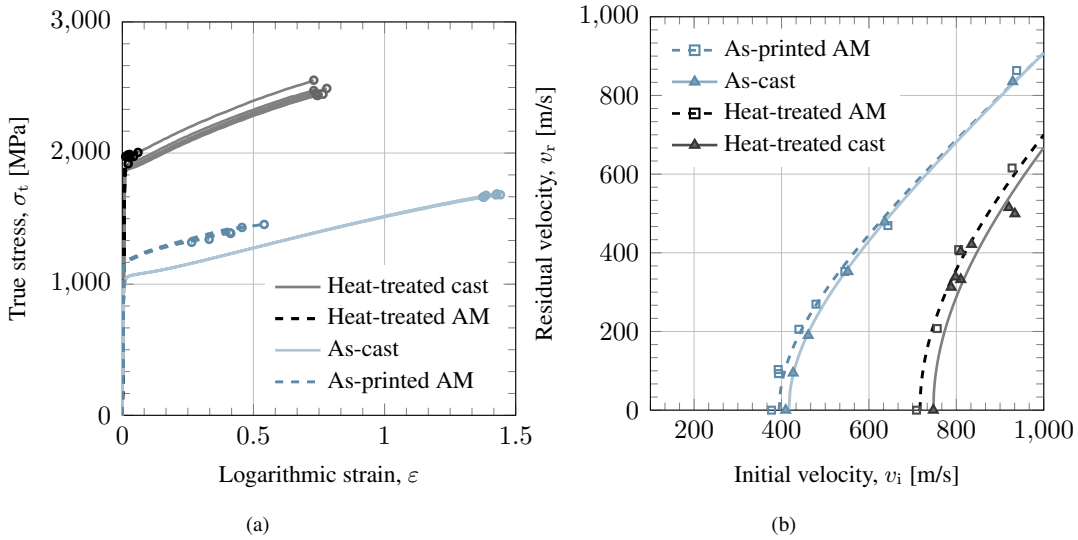

Figure 2. Experimental results: (a) tensile test results on cast and AM maraging steel, the latter specimens extracted in the AM build direction (b) Experimental ballistic test results on cast and AM maraging steel; heat-treated 2 × 5 mm plates and as-printed 1 × 5 mm plates, where the solid lines represent the fitted Recht-Ipson model.

test specimen fracture surfaces displayed in Figure 3. A dimpled surface pattern indicative of ductile failure upon the coalescence of voids is visible for cast maraging steel specimens in both the as-cast and heat-treated state in Figures 3b and 3d, respectively. The dimples of the heat-treated cast specimen surface appear to be shallower as a result of more brittle behaviour, in accordance with the reduction in strain at failure after heat-treatment found in the tensile tests. In contrast, the fracture surface of heat-treated AM specimen contains craters, cracks and cleavages typical of brittle fracture. The as-printed AM specimen exhibits dimples and holes as observed for the as-cast specimen, however with a larger diameter and depth. In Figure 3a, a hole has been identified containing a spherical particle of a diameter consistent with range expected of powder particles used during the AM build. Small spherical particles on the fracture surface and inside voids were not unique to the as-printed AM material: similar particles may be observed in Figure 3c of the heat-treated AM specimen. The latter indicates both the presence of unmelted powder particles inside the AM maraging steel that the heat-treatment process does not affect, other than that some particles in the heat-treated material appear to be fused together.

Ballistic Impact Tests

Figure 4 presents SEM images of the bullet perforation channel in an example ballistic test for each target configuration. Plastic deformation and evidence of smeared surfaces during temperature softening is apparent in both Figures 4a and 4b for the as-printed AM and as-cast material, respectively. Smooth surfaces and cracks characteristic of brittle fracture can be observed in Figures 4c and 4d for the heat-treated AM and cast material as a result of fragmentation in the target failure mode as opposed to ductile hole growth.

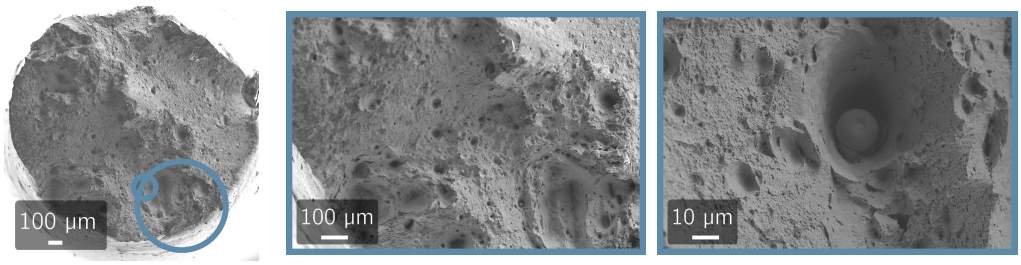

(a)

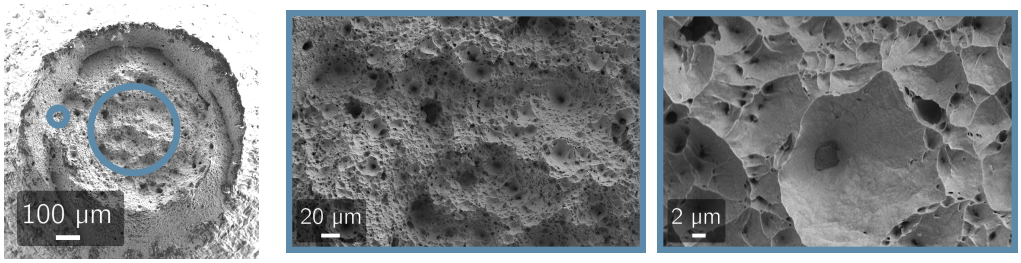

(b)

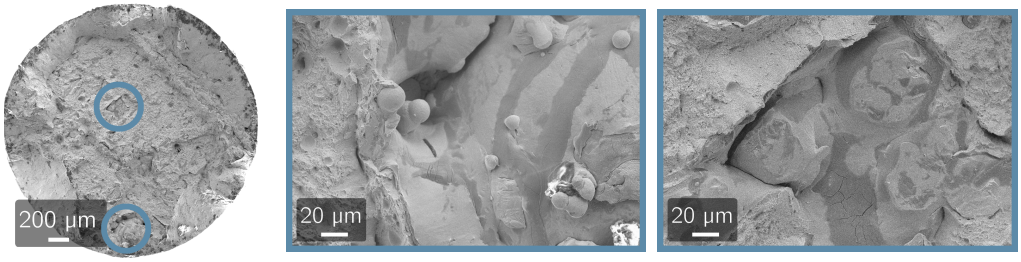

(c)

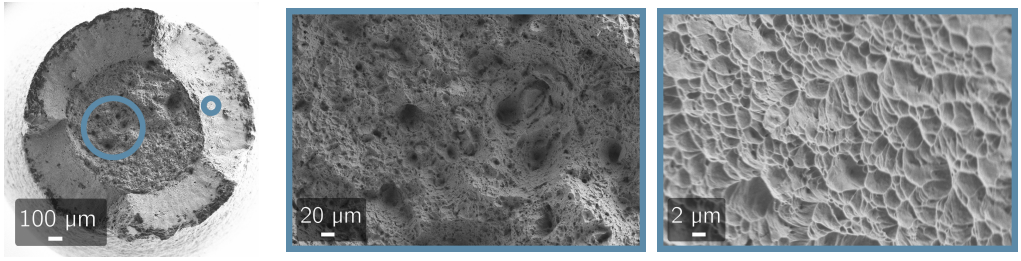

(d)

Figure 3. SEM images of quasi-static tensile test fracture surface of maraging steel: (a) as-printed AM, (b) heat-treated AM, (c) as-cast, (d) heat-treated cast.

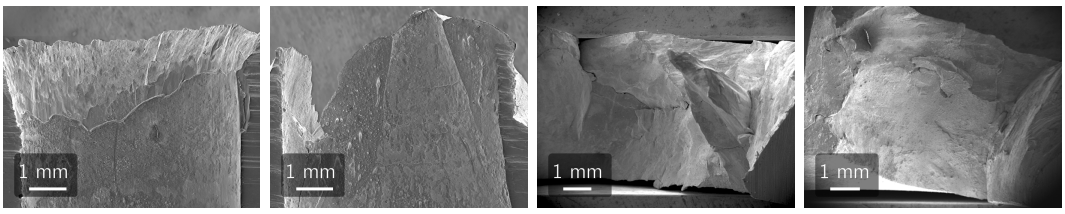

(a) (b) (c) (d)

Figure 4. SEM images of penetration channels from ballistic impact tests: (a) as-printed AM, (b) as-cast, (c) heat-treated AM, (d) heat-treated cast.

Snapshots of high-speed camera recordings for selected ballistic impact tests are displayed in Figures 5 and 6 for further analysis of the ballistic performance and perforation mechanisms. Similar behaviour during perforation was observed for AM and cast as-printed targets at both high velocities and low velocities, as exemplified in Figure 5. At impact velocities of around 930 m/s, shown in Figures 5a and 5b, both AM and cast targets experienced a similar amount of fragmentation and were unable to strip the copper jacket from the bullet core, resulting in a similar, albeit slightly larger, reduction in projectile velocity for cast compared to AM. At a low impact velocity of 392.4 m/s, the as-printed AM target strips the bullet of its copper jacket and fragments the tip of the core which perforates the plate along with small target plate fragments, as shown in Figure 5c. In Figure 5d the ballistic limit velocity of the as-cast target has been reached at 409.5 m/s: the projectile is arrested while the target experiences plastic deformation representative of ductile hole growth.

At high impact velocities fragmentation was observed for both the heat-treated AM and cast targets. The examples depicted in Figures 6a and 6b show broken bullet cores emerging from the AM and cast targets with a similar residual velocity alongside fragments of the maraging steel. Note that the case presented in Figure 6b is exceptional for the heat-treated cast targets being the only test out of eight during which the bullet core was damaged. On the contrary, fracture of the bullet core occurred in each of the four tests on the heat-treated AM material. At an impact velocity of roughly 900 m/s, the heat-treated AM target produced larger fragments than the cast target for which the residual bullet velocity was around 100 m/s lower. Despite more significant fragmentation of the target plate at higher velocities, the heat-treated AM target induced fragmentation of the steel bullet core whereas the cast target did not. At the respective ballistic limit velocities, both the AM and cast heat-treated targets were able to pulverise the bullet upon impact, in that no sizeable fragments can be identified from the high-speed camera images in Figures 6c and 6d.

Figure 7 presents photographs of the front side of both the front and back target plates for the same two ballistic impact tests on the heat-treated AM and cast maraging steel as the high-speed camera snapshots in Figure 6. The plates shown in Figure 7a of the 809.9 m/s impact velocity test demonstrate the severity of target fragmentation for the heat-treated AM material compared to the cast. The back plate for the AM target is fragmented into three pieces, whereas the cast target exhibits only a small central hole with significant plastic deformation of the bulk of the plate. A similar scenario may be observed in Figure 7b at the ballistic limit velocity; despite preventing perforation of the bullet or any fragments the heat-treated AM back plate has experienced a breakage, whereas that of the cast experienced only a small amount of damage and plastic deformation. The nature of the mechanism adopted by the second 5 mm plate in order to reach the ballistic limit velocity may also be inferred from Figure 7. For the heat-treated AM target, the projectile was unable to perforated the front plate: a feature which may have been facilitated by energy absorption during the breakage of the back plate. For the heat-treated cast target, the damage to the front of the back plate evidences that the front plate alone was incapable of preventing either perforation of the bullet, fragments of maraging steel, or both.

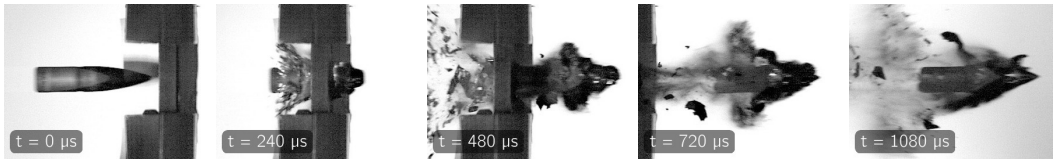

(a) As-printed AM v_{i} = 937.9 m/s; v_{r} = 863.4 m/s.

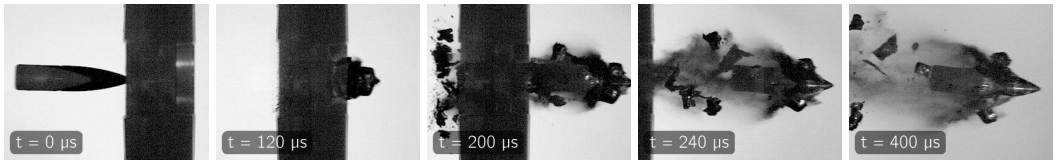

(b) As-printed cast v_{i} = 928.9 m/s; v_{r} = 835.2 m/s.

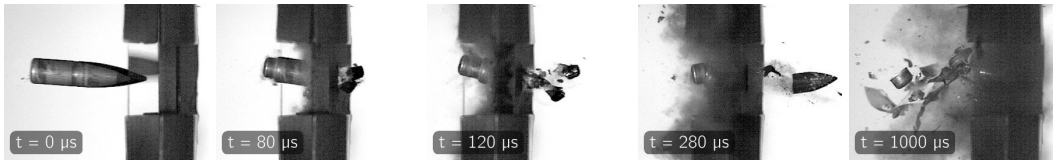

(c) As-printed AM v_{i} = 392.4 m/s; v_{r} = 103.3 m/s.

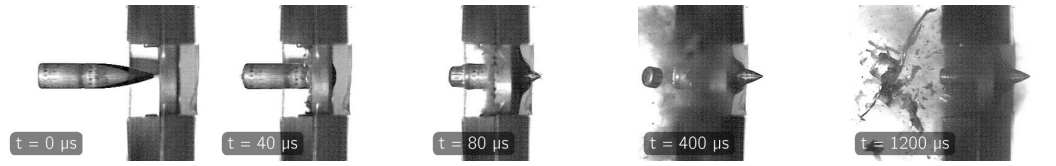

(d) As-printed cast v_{i} = 409.5 m/s; v_{r} = 0.0 m/s.

Figure 5. Sequential images of 1 $\times$ 5 mm as-printed target plates impacted by armour piercing bullets captured with a high-speed camera: (a) and (b) at higher velocities $\approx$ 930 m/s for AM and cast, respectively; (c) and (d) at lower velocities $\approx$ 400 m/s for AM and cast, respectively.

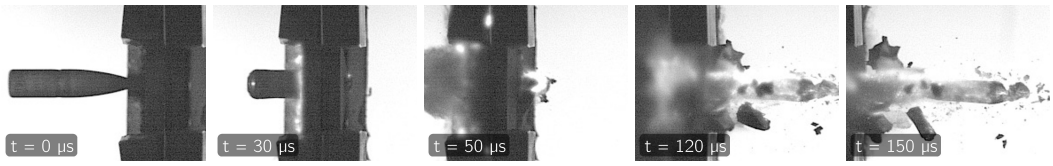

(a) Heated-treated AM v_i = 805.2 m/s; v_r = 408.1 m/s.

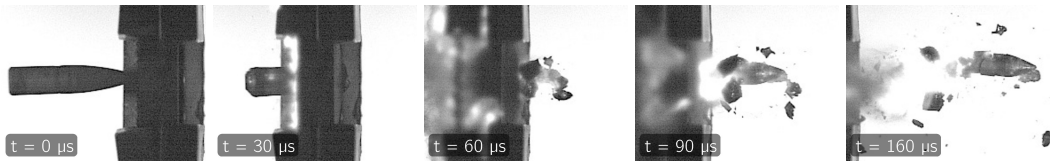

(b) Heated-treated cast v_i = 809.9 m/s; v_r = 403.0 m/s.

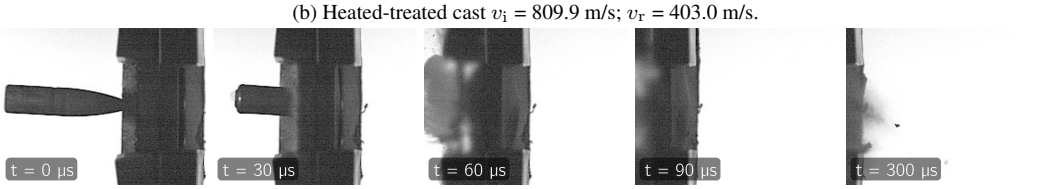

(c) Heated-treated AM v_i = 708.9 m/s; v_r = 0 m/s.

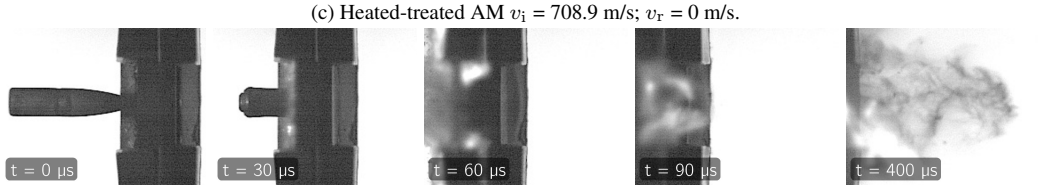

(d) Heated-treated cast v_i = 747.3 m/s; v_r = 0 m/s..

Figure 6. Sequential images of 2 × 5 mm heat-treated target plates impacted by armour piercing bullets captured with a high-speed camera: (a) and (b) at higher velocities ≈ 930 m/s for AM and cast, respectively; (c) and (d) at medium velocities ≈ 700–750 m/s for AM and cast, respectively.

(a) AM v_i = 805.2 m/s; v_r = 408.1 m/s and cast v_i = 809.9 m/s; v_r = 403.0 m/s.

(b) AM v_i = 708.9 m/s; v_r = 0 m/s and cast v_i = 747.3 m/s; v_r = 0 m/s.

Figure 7. Projectile-facing sides of the 2 × 5 mm heat-treated AM and cast target plates after ballistic impact tests. Comparisons are made at (a) high velocity and (b) ballistic limit velocity.

FINAL REMARKS

Findings of material properties for AM maraging steel fabricated by laser powder-bed fusion before and after heat-treatment were reasonably in agreement with the literature. A large increase in mechanical strength was observed for the maraging steel post heat-treatment as anticipated, with a 20% higher increase for the cast compared to the AM specimens. The effect of heat-treatment on the mechanical properties of AM maraging steel followed the expected trends based on an understanding of the material composition, however with some quantifiable differences. The results presented here are similar to some existing studies, Tan et al. [8] for example, but diverge from others. When compared to Costas et al. [11] the increase in AM maraging steel yield stress and ultimate tensile strength were around 20% smaller in the present work, while the decrease in strain at fracture was 30% larger.

The effects of AM processing compared to casting on the microstructure and resulting material properties were clarified through SEM imaging. Analysis of fracture surfaces reflected the differences in strain at fracture found in the tensile tests, specifically a reduction of approximately 48% and 93% in strain at fracture for the cast and AM maraging steel respectively. Dimples and holes in fracture surfaces of the as-printed AM and cast maraging steel where craters and cleavage fractures were found for the heat-treated AM material. Despite differences in material properties and perforation mechanisms, the overall discrepancy in estimated ballistic limit velocity between AM and cast was found to be within 5% both before and after heat-treatment.

Identified differences in brittle behaviour between AM and cast were clearly evident in high-speed camera visual analysis of the perforation processes. For the as-printed targets, more fragmentation was observed for the AM material with insignificant consequences at high velocities, where AM and cast residual bullet velocities were similar, but with a detrimental effect at low velocities where a lack of plastic deformation allowed perforation at higher velocities for the AM than cast. The slightly higher mechanical strength for the as-printed maraging steel compared to the as-cast did not lead to a higher ballistic limit for the former material. For the heat-treated targets, again more fragmentation was observed for the AM material but with additional fragmentation for the hard steel bullet core compared to the heat-treated cast material. The conclusion that heat-treating AM maraging steel leads to higher-strength and higher ballistic limit velocities concurrently with more severe fragmentation as reported in previous work [11] was also reflected in the present results.

CONCLUSIONS

- Significant differences in material characteristics between AM and cast maraging steel were identified and may be attributed to the microstructure induced by laser powder-bed fusion.
- Despite a dramatic increase in brittle behaviour after heat-treatment for the AM maraging steel, very minimal differences in ballistic limit velocity were found between AM and cast targets.
- The heat-treated AM maraging steel demonstrated the best capacity of all target configurations for fracturing the hard steel armour piercing bullet core.

REFERENCES

[1] A.E. Medvedev, T. Maconachie, M. Leary, M. Qian, and M. Brandt. Perspectives on additive manufacturing for dynamic impact applications. Materials & Design, 221:110963, 2022.

[2] T.D. Ngo, A. Kashani, G. Imbalzano, K.T. Nguyen, and D. Hui. Additive manufacturing (3d printing): A review of materials, methods, applications and challenges. Composites Part B: Engineering, 143:172–196, 2018.

[3] M. Kristoffersen, M. Costas, T. Koenis, V. Brøtan, C.O. Paulsen, and T. Børvik. On the ballistic perforation resistance of additive manufactured alsi10mg aluminium plates. International Journal of Impact Engineering, 137:103476, 2020.

[4] A.E. Medvedev, E.W. Lui, D. Edwards, M. Leary, M. Qian, and M. Brandt. Improved ballistic performance of additively manufactured ti6al4v with $\alpha - \beta$ lamellar microstructures. Materials Science and Engineering: A, 825:141888, 2021.

[5] E.W. Lui, A.E. Medvedev, D. Edwards, M. Qian, M. Leary, and M. Brandt. Microstructure modification of additive manufactured ti-6al-4v plates for improved ballistic performance properties. Journal of Materials Processing Technology, 301:117436, 2022.

[6] B. Mooney, K.I. Kourousis, and R. Raghavendra. Plastic anisotropy of additively manufactured maraging steel: Influence of the build orientation and heat treatments. Additive Manufacturing, 25:19–31, 2019.

[7] Y. Bai, Y. Yang, D. Wang, and M. Zhang. Influence mechanism of parameters process and mechanical properties evolution mechanism of maraging steel 300 by selective laser melting. Materials Science and Engineering: A, 703:116–123, 2017.

[8] C. Tan, K. Zhou, W. Ma, P. Zhang, M. Liu, and T. Kuang. Microstructural evolution, nanoprecipitation behavior and mechanical properties of selective laser melted high-performance grade 300 maraging steel. Materials & Design, 134:23–34, 2017.

[9] T. Børvik, S. Dey, and A. Clausen. Perforation resistance of five different high-strength steel plates subjected to small-arms projectiles. International Journal of Impact Engineering, 36(7):948–964, 2009.

[10] T. Fras, C.C. Roth, and D. Mohr. Dynamic perforation of ultra-hard high-strength armor steel: Impact experiments and modeling. International Journal of Impact Engineering, 131:256–271, 2019.

[11] M. Costas, M. Edwards-Mowforth, M. Kristoffersen, F. Teixeira-Dias, V. Brøtan, C.O. Paulsen, and T. Børvik. Ballistic impact resistance of additive manufactured high-strength maraging steel: An experimental study. International Journal of Protective Structures, 12(4):577–603, aug 2021.

[12] J. Holmen, J. Johnsen, S. Jupp, O. Hopperstad, and T. Børvik. Effects of heat treatment on the ballistic properties of aa6070 aluminium alloy. International Journal of Impact Engineering, 57:119–133, 2013.

[13] Y. Bai, D. Wang, Y. Yang, and H. Wang. Effect of heat treatment on the microstructure and mechanical properties of maraging steel by selective laser melting. Materials Science and Engineering: A, 760:105–117, 2019.

[14] Abrams Industries. Abrams steel. `https://eu.abrams-industries.com/steel/`, 2023.

[15] E. Fagerholt, T. Børvik, and O. Hopperstad. Measuring discontinuous displacement fields in cracked specimens using digital image correlation with mesh adaptation and crack-path optimization. Optics and Lasers in Engineering, 51(3):299–310, 2013.

[16] R.F. Recht and T.W. Ipson. Ballistic perforation dynamics. International Journal of Applied Mechanics (Trans ASME), 30:384–390, sep 1963.